

A Versatile Precursor for the Synthesis of New Ruthenium Olefin Metathesis Catalysts

Melanie S. Sanford, Jennifer A. Love, and Robert H. Grubbs*

Arnold and Mabel Beckman Laboratories for Chemical Synthesis, Division of Chemistry and Chemical Engineering, California Institute of Technology, Pasadena, California 91125

Received July 5, 2001

The ruthenium complex $(\text{IMesH}_2)(\text{Cl})_2(\text{C}_5\text{H}_5\text{N})_2\text{Ru}=\text{CHPh}$ [$\text{IMesH}_2 = 1,3\text{-dimesityl-4,5-dihydroimidazol-2-ylidene}$] (**3**) was prepared by the reaction of $(\text{IMesH}_2)(\text{PCy}_3)(\text{Cl})_2\text{Ru}=\text{CHPh}$ (**2**) with an excess of pyridine. Complex **3** contains substitutionally labile pyridine and chloride ligands and serves as a versatile starting material for the synthesis of new ruthenium benzylidenes.

Introduction

Olefin metathesis is a carbon–carbon bond-forming reaction that is widely used in both organic and polymer chemistry.¹ In particular, the ruthenium-based metathesis catalyst $(\text{PCy}_3)_2(\text{Cl})_2\text{Ru}=\text{CHPh}$ (**1**) (Figure 1)² has been employed for the construction of small molecules, macromolecular architectures, and natural products in the presence of most common functional groups.³ Recently, *N*-heterocyclic carbene (NHC) coordinated ruthenium alkylidenes,^{4–6} particularly $(\text{IMesH}_2)(\text{PCy}_3)(\text{Cl})_2\text{Ru}=\text{CHPh}$ (**2**) [$\text{IMesH}_2 = 1,3\text{-dimesityl-4,5-dihydroimidazol-2-ylidene}$],⁷ have been introduced and shown to exhibit dramatically increased olefin metathesis activity relative to **1**.^{7,8} Mechanistic studies of **2** and the related complexes $(\text{IMesH}_2)(\text{PR}_3)(\text{X})_2\text{Ru}=\text{CHR}^1$ have revealed that the ancillary ligands dramatically affect the rates of initiation and propagation in olefin metathesis reactions.^{9a,10} As a result, significant current effort is focused on modification of the ligand environment of **2** in order to produce new metathesis catalysts with improved stability, activity, selectivity, and functional

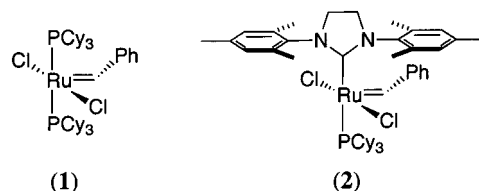


Figure 1. Ruthenium olefin metathesis catalysts.

group tolerance. This report describes the synthesis, characterization, and reactivity of a new ruthenium benzylidene, $(\text{IMesH}_2)(\text{Cl})_2(\text{C}_5\text{H}_5\text{N})_2\text{Ru}=\text{CHPh}$ (**3**), which contains substitutionally labile pyridine and chloride ligands. Complex **3** serves as a versatile starting material for the preparation of structurally diverse ruthenium olefin metathesis catalysts.

Results and Discussion

The reaction of complex **2** with a large excess (~100 equiv) of pyridine results in a rapid color change from red to bright green, and transfer of the resulting solution to cold ($-10\text{ }^\circ\text{C}$) pentane leads to the precipitation of the bis-pyridine adduct $(\text{IMesH}_2)(\text{Cl})_2(\text{C}_5\text{H}_5\text{N})_2\text{Ru}=\text{CHPh}$ (**3**) (Scheme 1).¹¹ Complex **3** can be purified by several washes with pentane and is isolated as an air-stable green solid that is soluble in CH_2Cl_2 , benzene, and THF. This procedure provides **3** in 80–85% yield and is easily carried out on a multigram scale.

Crystals suitable for X-ray crystal structure determination were grown by vapor diffusion of pentane into a saturated benzene solution of **3** at room temperature.¹² The collection and refinement parameters for the crystallographic analysis are summarized in Table 1. A

(10) For a recent study detailing ligand modifications and comparative reactivity data for ruthenium-based complexes bearing NHC ligands, see: Fürstner, A.; Ackermann, L.; Gabor, B.; Goddard, R.; Lehmann, C. W.; Mynott, R.; Stelzer, F.; Thiel, O. R. *Chem. Eur. J.* **2001**, *7*, 3236.

(11) An analogous procedure has been used to produce the phosphine analogue of **3**, $[(\text{PCy}_3)(\text{Cl})_2(\text{C}_5\text{H}_5\text{N})_2\text{Ru}=\text{CHPh}]$, from catalyst **1**. Dias, E. L., Ph.D. Thesis, California Institute of Technology, Pasadena, CA, 1997.

(12) Two independent (but very similar) molecules of **3** appear in the asymmetric unit, and the bond lengths and angles for molecule B are reported. Molecule B has somewhat smaller displacement ellipsoids (and smaller errors associated with bond distances and angles) than molecule A.

(1) Ivin, K. J.; Mol, J. C. *Olefin Metathesis and Metathesis Polymerization*; Academic Press: San Diego, CA, 1997.

(2) Schwab, P.; Grubbs, R. H.; Ziller, J. W. *J. Am. Chem. Soc.* **1996**, *118*, 100.

(3) For recent reviews on applications of catalysts **1** and **2** in organic and polymer chemistry, see: (a) Trnka, T. M.; Grubbs, R. H. *Acc. Chem. Res.* **2001**, *34*, 18. (b) Fürstner, A. *Angew. Chem., Int. Ed.* **2000**, *39*, 3012. (c) Grubbs, R. H.; Chang, S. *Tetrahedron* **1998**, *54*, 4413.

(4) Scholl, M.; Trnka, T. M.; Morgan, J. P.; Grubbs, R. H. *Tetrahedron Lett.* **1999**, *40*, 2247.

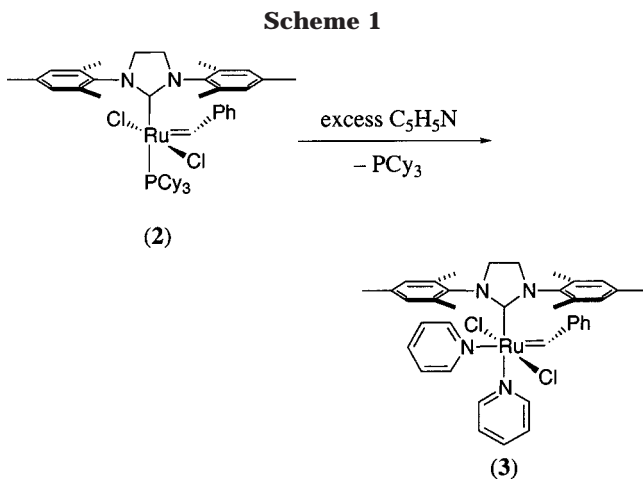
(5) (a) Jafarpour, L.; Stevens, E. D.; Nolan, S. P. *J. Organomet. Chem.* **2000**, *606*, 49. (b) Huang, J.; Schanz, H. J.; Stevens, E. D.; Nolan, S. P. *Organometallics* **1999**, *18*, 5375. (c) Jafarpour, L.; Schanz, H. J.; Stevens, E. D.; Nolan, S. P. *Organometallics* **1999**, *18*, 5416. (d) Schanz, H. J.; Jafarpour, L.; Stevens, E. D.; Nolan, S. P. *Organometallics* **1999**, *18*, 5187. (e) Huang, J.; Stevens, E. D.; Nolan, S. P.; Peterson, J. L. *J. Am. Chem. Soc.* **1999**, *121*, 2674.

(6) (a) Weskamp, T.; Kohl, F. J.; Hieringer, W.; Gleich, D.; Herrmann, W. A. *Angew. Chem., Int. Ed. Engl.* **1999**, *38*, 2416. (b) Weskamp, T.; Kohl, F. J.; Herrmann, W. A. *J. Organomet. Chem.* **1999**, *582*, 362.

(7) Scholl, M.; Ding, S.; Lee, C. W.; Grubbs, R. H. *Org. Lett.* **1999**, *1*, 953.

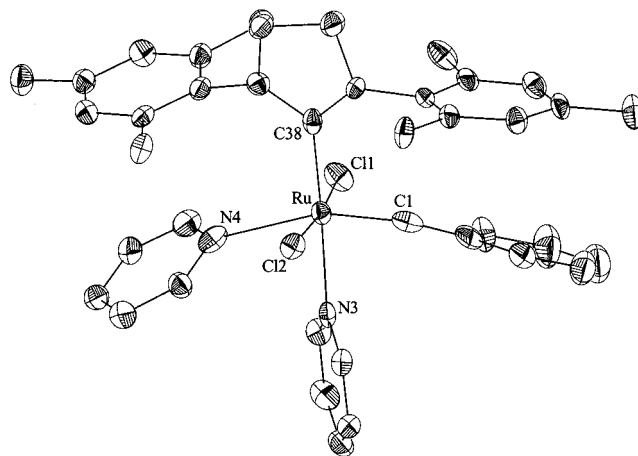
(8) (a) Choi, T.-L.; Chatterjee, A. K.; Grubbs, R. H. *Angew. Chem., Int. Ed.* **2001**, *40*, 1277. (b) Chatterjee, A. K.; Morgan, J. P.; Scholl, M.; Grubbs, R. H. *J. Am. Chem. Soc.* **2000**, *122*, 3783. (c) Bielawski, C. W.; Grubbs, R. H. *Angew. Chem., Int. Ed.* **2000**, *39*, 2903.

(9) (a) Sanford, M. S.; Love, J. A.; Grubbs, R. H. *J. Am. Chem. Soc.* **2001**, *123*, ASAP article. (b) Sanford, M. S.; Ulman, M.; Grubbs, R. H. *J. Am. Chem. Soc.* **2001**, *123*, 749.

**Table 1. Crystal Data and Structure Refinement for Complex 3**

empirical formula	C ₇₆ H ₈₄ Cl ₄ N ₈ Ru ₂
formula weight	1453.46
crystal habit	rod
crystal size	0.41 × 0.11 × 0.07 mm ³
crystal color	emerald green
diffractometer	CCD area detector
wavelength	0.71073 Mo K α
temperature	98 K
unit cell dimensions	$a = 12.3873(16) \text{ \AA}$ $b = 15.529(2) \text{ \AA}$ $c = 18.562(2) \text{ \AA}$ $\alpha = 78.475(2)^\circ$ $\beta = 81.564(2)^\circ$ $\gamma = 76.745(2)^\circ$
volume	3386.2(8) \AA^3
Z	4
crystal system	Triclinic
space group	P1
density (calculated)	2.758 Mg/m ³
θ range	1.61–28.51 $^\circ$
h min, max	–16, 16
k min, max	–20, 20
l min, max	–24, 24
reflections collected	76469
independent reflections	15655
GOF on F^2	1.438
R_{int}	0.867
final R indices [$I > 2\sigma(I)$]	0.0609
final weighted R (F_o^2)	0.0855

labeled view of **3** is shown in Figure 2, and representative bond lengths and bond angles are reported in Table 2. Several structural isomers of the bis-pyridine adduct can be envisioned, but the solid-state structure reveals that the pyridines bind in a cis geometry, occupying the coordination sites trans to the benzylidene and the *N*-heterocyclic carbene ligand. The Ru=C(1) (benzylidene carbon) bond length of 1.873(4) \AA is slightly longer than those in five-coordinate ruthenium olefin metathesis catalysts, including **1** [$d(\text{Ru}=\text{C}_\alpha) = 1.838(2) \text{ \AA}$]¹³ and **2** [$d(\text{Ru}=\text{C}_\alpha) = 1.835(2) \text{ \AA}$].¹⁴ The elongated Ru=C α bond in **3** likely results from the presence of a trans pyridine ligand.¹⁵ The Ru–C(38) (*N*-heterocyclic

**Figure 2.** Labeled view of complex **3** with 50% probability ellipsoids.**Table 2. Selected Bond Lengths (\AA) and Angles (deg) for Complex 3**

Bond Lengths (\AA)			
Ru–C(1)	1.873(4)	Ru–C(38)	2.033(4)
Ru–N(3)	2.203(3)	Ru–N(4)	2.372(4)
Ru–Cl(1)	2.3995(12)	Ru–Cl(2)	2.4227(12)
Bond Angles (deg)			
C(38)–Ru–C(1)	93.61(17)	C(1)–Ru–N(3)	87.07(15)
C(38)–Ru–N(3)	176.40(14)	C(1)–Ru–N(4)	161.18(14)
C(38)–Ru–N(4)	102.85(14)	C(1)–Ru–Cl(1)	100.57(14)
C(38)–Ru–Cl(1)	93.83(12)	C(1)–Ru–Cl(2)	84.75(14)
C(38)–Ru–Cl(2)	84.39(11)	Cl(1)–Ru–Cl(2)	174.50(4)

carbene) bond length of 2.033(4) \AA is approximately 0.05 \AA shorter than that in complex **2**,¹⁴ which is likely due to the relatively small size and moderate trans influence of pyridine relative to PCy₃. The 0.15 \AA difference in the Ru–C(1) and Ru–C(38) bond distances highlights the covalent nature of the former and the dative nature of the latter ruthenium–carbene bond. Interestingly, the two Ru–N bond distances differ by more than 0.15 \AA , indicating that the benzylidene ligand exerts a significantly larger trans influence than the *N*-heterocyclic carbene.¹⁶

The kinetics of the reaction between **2** and pyridine was investigated in order to determine the mechanism of this ligand substitution. The reaction of **2** (0.88 M in toluene) with an excess of pyridine-*d*₅ (0.18–0.69 M) is accompanied by a 150-nm red shift of the visible MLCT absorbance,^{9a} and this transformation can be followed by UV–vis spectroscopy. The disappearance of starting material (502 nm) was monitored at 20 $^\circ\text{C}$, and in all cases, the data fit first-order kinetics over five half-lives. A plot of k_{obs} versus $[\text{C}_5\text{D}_5\text{N}]$ is presented in Figure 3. The data show an excellent linear fit ($R^2 = 0.999$) even at high concentrations of pyridine, and the y -intercept of this line (1.1×10^{-3}) is very close to zero. The rate constant for phosphine dissociation (k_{B}) in complex **2** has been determined independently by ³¹P magnetization transfer experiments, and at 20 $^\circ\text{C}$, k_{B} is $4.1 \times 10^{-5} \text{ s}^{-1}$.⁹ This value of k_{B} places an upper limit on the rate of dissociative ligand exchange in **2**, and the observed rate constants for pyridine substitution are clearly 3 orders of magnitude larger than k_{B} . Taken

(13) Trnka, T. M.; Henling, L. M.; Day, M. W.; Grubbs, R. H. **2000**, unpublished results.

(14) Sanford, M. S.; Henling, L. M.; Grubbs, R. H. **2000**, unpublished results.

(15) Octahedral ruthenium alkylidenes typically have Ru–C α distances of approximately 1.87 \AA . For example, see: (a) Sanford, M. S.; Henling, L. M.; Grubbs, R. H. *Organometallics* **1998**, *17*, 5384. (b) Leung, W.-A.; Lau, K.-K.; Zhang, Q.-F.; Wong, W.-T.; Tang, B. *Organometallics* **2000**, *19*, 2084. (c) Esteruelas, M. A.; Lahoz, F. J.; Onate, E.; Oro, L. A.; Zeier, B. *Organometallics* **1994**, *13*, 4258.

(16) The large trans influence of the Ru=CHPh moiety has been noted in the tris(pyrazolyl)borate complex $[\text{Tp}(\text{PCy}_3)(\text{H}_2\text{O})\text{-Ru}=\text{CHPh}]\text{BF}_4$ (ref 15a).

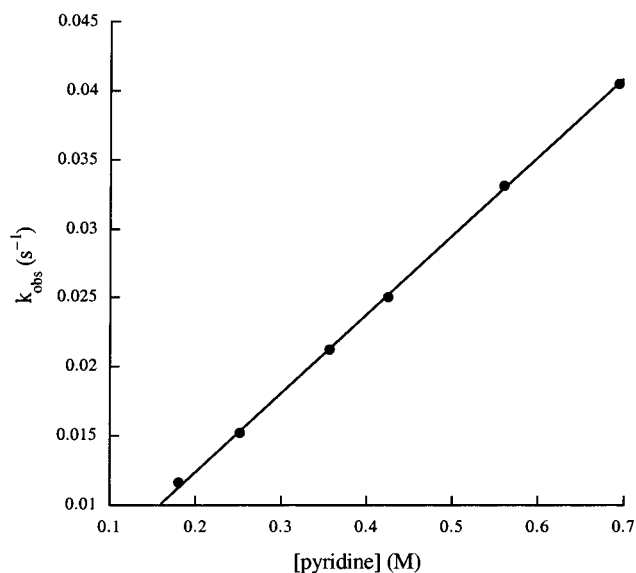


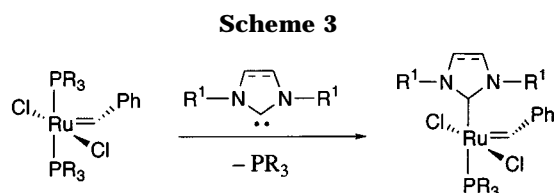
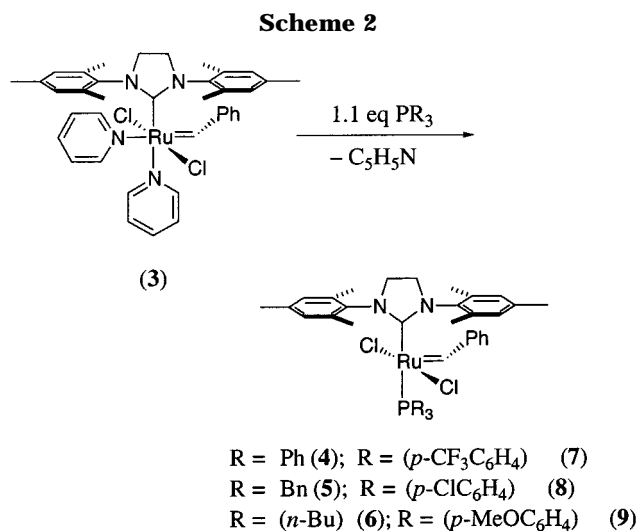
Figure 3. Plot of k_{obs} versus $[\text{C}_5\text{D}_5\text{N}]$ for the reaction of **2** with $\text{C}_5\text{D}_5\text{N}$.

together, these results indicate that the substitution of PCy_3 with pyridine proceeds by an associative mechanism with a second-order rate constant of $5.7 \times 10^{-2} \text{ M}^{-1} \text{ s}^{-1}$ at 20°C . In marked contrast, displacement of the phosphine ligand of **2** with olefinic substrates (which is the initiation event in olefin metathesis reactions) occurs via a dissociative mechanism.¹⁹

Initial reactivity studies of complex **3** revealed that both pyridine ligands are substitutionally labile. For example, benzylidene **3** reacts instantaneously with 1.1 equiv of PCy_3 to release pyridine and regenerate complex **2**. This equilibrium can be driven back toward the pyridine adduct by addition of an excess of $\text{C}_5\text{D}_5\text{N}$, but it is readily reestablished by removal of the volatiles under vacuum.

The facile reaction of **3** with PCy_3 suggested that the pyridines might be displaced by other incoming ligands, and we have found that reaction of the bis-pyridine complex with a wide variety of phosphines provides a simple and divergent route to new ruthenium benzylidenes of the general formula $(\text{IMesH}_2)(\text{PR}_3)(\text{Cl})_2\text{Ru}=\text{CHPh}$. The combination of **3** and 1.1 equiv of PR_3 results in a color change from green to red/brown and formation of the corresponding PR_3 adduct. The residual pyridine can be removed under vacuum, and the ruthenium products are purified by several washes with pentane and/or by column chromatography. This ligand substitution works well for a variety of alkyl- and aryl-substituted phosphines including PPh_3 , PBn_3 , and $\text{P}(n\text{-Bu})_3$ to produce complexes **4**, **5**, and **6**, respectively (Scheme 2). Additionally, the para-substituted triphenylphosphine derivatives **7–9** (containing para substituents CF_3 , Cl , and OMe , respectively) can be prepared using this methodology. The synthetic accessibility of complex **7** is particularly remarkable, because $\text{P}(p\text{-CF}_3\text{C}_6\text{H}_4)_3$ is an extremely electron-poor phosphine ($\chi = 20.5 \text{ cm}^{-1}$).¹⁷ The triarylphosphine ruthenium complexes **4** and **7–9** are valuable catalysts as they are almost 2 orders of magnitude more active for olefin metathesis reactions than the parent complex **2**.^{9,18,19}

There appear to be both steric and electronic limitations on the incoming phosphine ligand in the pyridine



substitution reaction. For example, complex **3** does not react with $\text{P}(o\text{-tolyl})_3$ to produce a stable product, presumably due to the prohibitive size of the incoming ligand.²⁰ The cone angle of $\text{P}(o\text{-tolyl})_3$ is 194° , while that of PCy_3 (the largest phosphine shown to successfully displace the pyridines of **3**) is 170° .²⁰ Additionally, the electron-poor phosphine $\text{P}(\text{C}_6\text{F}_5)_3$ shows no reaction with **3**, even under forcing conditions. This ligand has a significantly lower electron donor capacity ($\chi = 33.6 \text{ cm}^{-1}$) than $\text{P}(p\text{-CF}_3\text{C}_6\text{H}_4)_3$ ($\chi = 20.5 \text{ cm}^{-1}$)¹⁷ and also has a larger cone angle than PCy_3 ($\Theta = 184^\circ$).²⁰

The methodology described herein represents a dramatic improvement over previous synthetic routes to the complexes $(\text{NHC})(\text{PR}_3)(\text{Cl})_2\text{Ru}=\text{CHPh}$. As shown in Scheme 3, earlier preparations of these compounds involved reaction of the bis-phosphine precursor $(\text{PR}_3)_2(\text{Cl})_2\text{Ru}=\text{CHPh}$ with an NHC ligand.^{21,22} These transformations were often low yielding (particularly when the NHC was small),²² and required the parallel synthesis of ruthenium precursors containing each PR_3 ligand. Furthermore, bis-phosphine starting materials containing PR_3 ligands that are smaller and less electron donating than PPh_3 ($\Theta = 145^\circ$; $\chi = 13.25 \text{ cm}^{-1}$; $\text{p}K_a = 2.73$)^{17,20,23} cannot be prepared,^{24,25} placing severe limitations on the complexes that are available by the procedure outlined in Scheme 3.

(17) Wilson, M. R.; Woska, D. C.; Prock, A.; Giering, W. P. *Organometallics* **1993**, *12*, 1742.

(18) Complex **3** is an active initiator for olefin metathesis; this activity is currently being investigated further.

(19) Love, J. A.; Grubbs, R. H. Unpublished results, 2001.

(20) Tolman, C. A. *Chem. Rev.* **1977**, *77*, 113.

(21) Huang, J.; Stevens, E. D.; Nolan, S. P.; Peterson, J. L. *J. Am. Chem. Soc.* **1999**, *121*, 2674.

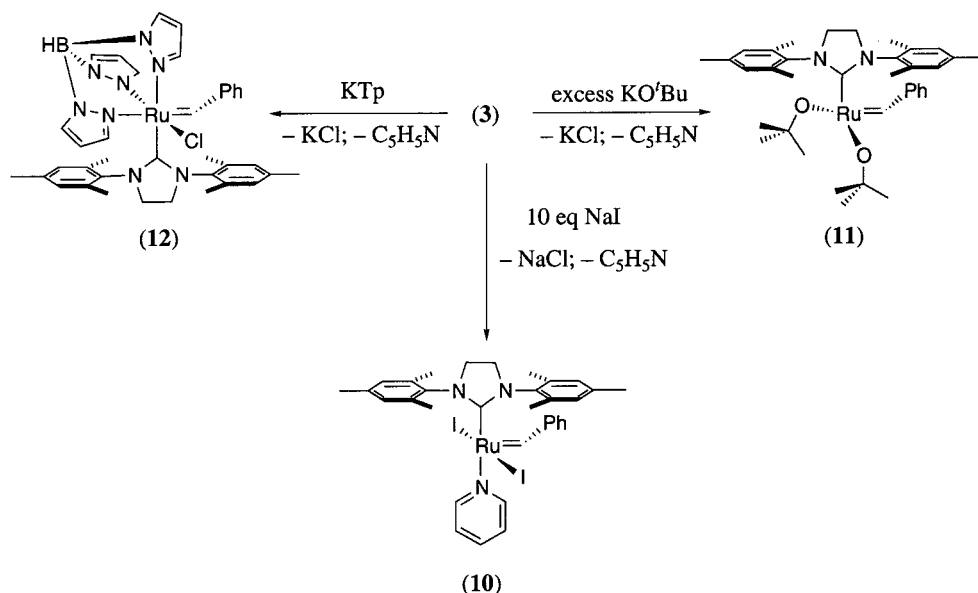
(22) Weskamp, T.; Kohl, F. J.; Herrmann, W. A. *J. Organomet. Chem.* **1999**, *582*, 362.

(23) Streuli, C. A. *Anal. Chem.* **1960**, *32*, 985.

(24) Nguyen, S. T., Ph.D. Thesis, California Institute of Technology, Pasadena, CA, 1995.

(25) Cucullu, M. E.; Li, C.; Nolan, S. P.; Nguyen, S. T.; Grubbs, R. H. *Organometallics* **1998**, *17*, 5565.

Scheme 4



The chloride ligands of **3** are also substitutionally labile relative to those in the parent complex **2**. For example, **3** reacts quantitatively with NaI within 2 h at room temperature to afford $(\text{IMesH}_2)(\text{I})_2(\text{C}_5\text{H}_5\text{N})\text{-Ru}=\text{CHPh}$ (**10**) (Scheme 4). In contrast, the reaction between **2** and NaI takes approximately 8 h to reach completion under identical conditions.^{9a} Interestingly, ¹H NMR spectroscopy reveals that the diiodide complex **10** contains only one pyridine ligand, while the analogous dichloride species (**3**) coordinates 2 equiv of pyridine. The relatively large size of the iodide ligands and the lower electrophilicity at the metal center in **10** (as compared to **3**) are both believed to contribute to the formation of a five-coordinate complex in this system.

Complex **3** also reacts quantitatively with KTp [Tp = tris(pyrazolyl)borate] within 1 h at 25 °C to produce the bright green product $\text{Tp}(\text{IMesH}_2)(\text{Cl})\text{Ru}=\text{CHPh}$ (**12**) (Scheme 4), while the analogous reaction between complex **2** and KTp is extremely slow. (The latter proceeds to less than 50% completion even after several days at room temperature.) Removal of the solvents under vacuum followed by filtration and several washes with pentane and methanol provides **12** as an air and moisture stable solid. Preliminary ¹H NMR studies also show that the combination of **3** with an excess of KO^tBu produces the four-coordinate benzylidene, $(\text{IMesH}_2)(\text{O}^t\text{Bu})_2\text{Ru}=\text{CHPh}$ (**11**), quantitatively within 10 min at ambient temperature (Scheme 4). In contrast, the reaction between **2** and KO^tBu to form **11** does not proceed to completion, even after several days at 35 °C. Complex **11** may be considered a model for the 14-electron intermediate, $(\text{IMesH}_2)(\text{Cl})_2\text{Ru}=\text{CHPh}$, involved in olefin metathesis reactions of **2**.²⁶

In summary, this report describes a simple and high-yielding procedure for the preparation of $(\text{IMesH}_2)(\text{Cl})_2(\text{C}_5\text{H}_5\text{N})_2\text{Ru}=\text{CHPh}$ (**3**) from $(\text{IMesH}_2)(\text{Cl})_2(\text{PCy}_3)\text{-Ru}=\text{CHPh}$ (**2**). In contrast to the reaction of **2** with olefinic substrates, this ligand substitution proceeds by an associative mechanism. Complex **3** reacts readily with phosphines, providing access to new complexes of the general formula $(\text{IMesH}_2)(\text{Cl})_2(\text{PR}_3)\text{Ru}=\text{CHPh}$. Complex **3** also undergoes reaction with KO^tBu , NaI, and

KTp to provide new four-, five-, and six-coordinate ruthenium benzylidenes. In general, we anticipate that the synthetic methodology described herein will facilitate the development of new ruthenium olefin metathesis catalysts containing structurally diverse ligand arrays.

Experimental Section

General Procedures. Manipulation of organometallic compounds was performed using standard Schlenk techniques under an atmosphere of dry argon or in a nitrogen-filled Vacuum Atmospheres drybox ($\text{O}_2 < 2$ ppm). NMR spectra were recorded on a Varian Inova (499.85 MHz for ¹H; 202.34 MHz for ³¹P; 125.69 MHz for ¹³C) or a Varian Mercury 300 (299.817 MHz for ¹H; 121.39 MHz for ³¹P; 74.45 MHz for ¹³C). ³¹P NMR spectra were referenced using H_3PO_4 ($\delta = 0$ ppm) as an external standard. UV-vis spectra were recorded on an HP 8452A diode-array spectrophotometer. A detailed discussion of the NMR data for several of these and related complexes will be presented in a subsequent publication.²⁷

Materials and Methods. Pentane, toluene, benzene, and benzene-*d*₆ were dried by passage through solvent purification columns.²⁸ Pyridine was dried by vacuum transfer from CaH_2 . All phosphines as well as KTp were obtained from commercial sources and used as received. Ruthenium complex **2** was prepared according to literature procedures.^{7,9b}

$(\text{IMesH}_2)(\text{C}_5\text{H}_5\text{N})_2(\text{Cl})_2\text{Ru}=\text{CHPh}$ (3**).** Complex **2** (4.0 g, 4.7 mmol) was dissolved in toluene (10 mL), and pyridine (30 mL, 0.37 mol) was added. The reaction was stirred for 10 min during which time a color change from red to bright green was observed. The reaction mixture was cannula transferred into 100 mL of cold (-10 °C) pentane, and a green solid precipitated. The precipitate was filtered, washed with 4×50 mL of pentane, and dried under vacuum to afford **3** as a green powder (2.9 g, 85% yield). Samples for elemental analysis were prepared by recrystallization from C_6H_6 /pentane followed by drying under vacuum. These samples analyze as the monopyridine adduct $(\text{IMesH}_2)(\text{C}_5\text{H}_5\text{N})(\text{Cl})_2\text{Ru}=\text{CHPh}$, probably due

(26) Sanford, M. S.; Henling, L. M.; Day, M. W.; Grubbs, R. H. *Angew. Chem., Int. Ed.* **2000**, *39*, 3451.

(27) Sanford, M. S.; Trnka, T. M.; Love, J. A.; Grubbs, R. H., manuscript in preparation.

(28) Pangborn, A. B.; Giardello, M. A.; Grubbs, R. H.; Rosen, R. K.; Timmers, F. J. *Organometallics* **1996**, *15*, 1518.

to loss of pyridine under vacuum. ^1H NMR (C_6D_6): δ 19.67 (s, 1H, *CHPh*), 8.84 (br. s, 2H, pyridine), 8.39 (br. s, 2H, pyridine), 8.07 (d, 2H, ortho *CH*, $J_{\text{HH}} = 8$ Hz), 7.15 (t, 1H, para *CH*, $J_{\text{HH}} = 7$ Hz), 6.83–6.04 (br. multiple peaks, 9H, pyridine, Mes *CH*), 3.37 (br. d, 4H, CH_2CH_2), 2.79 (br. s, 6H, Mes CH_3), 2.45 (br. s, 6H, Mes CH_3), 2.04 (br. s, 6H, Mes CH_3). $^{13}\text{C}\{^1\text{H}\}$ NMR (C_6D_6): δ 314.90 (m, Ru=*CHPh*), 219.10 (s, Ru- $\text{C}(\text{N})_2$), 152.94, 150.84, 139.92, 138.38, 136.87, 135.99, 134.97, 131.10, 130.11, 129.88, 128.69, 123.38, 51.98, 51.37, 21.39, 20.96, 19.32. Anal. Calcd for $\text{C}_{33}\text{H}_{37}\text{N}_3\text{Cl}_2\text{Ru}$: C, 61.20; H, 5.76; N, 6.49. Found: C, 61.25; H, 5.76; N, 6.58.

Representative Synthesis of a Phosphine Complex: (IMesH₂)(PPh₃)(Cl)₂Ru=CHPh (4). Complex **3** (150 mg, 0.21 mmol) and PPh₃ (76 mg, 0.28 mmol) were combined in benzene (10 mL) and stirred for 10 min. The solvent was removed under vacuum, and the resulting brown residue was washed with 4 × 20 mL of pentane and dried in vacuo. Complex **4** was obtained as a brownish powder (125 mg, 73% yield). $^{31}\text{P}\{^1\text{H}\}$ NMR (C_6D_6): δ 37.7 (s). ^1H NMR (C_7D_8): δ 19.60 (s, 1H, Ru=*CHPh*), 7.70 (d, 2H, ortho *CH*, $J_{\text{HH}} = 8$ Hz), 7.29–6.71 (multiple peaks, 20H, PPh₃, para *CH*, meta *CH*, and Mes *CH*), 6.27 (s, 2H, Mes *CH*), 3.39 (m, 4H, CH_2CH_2), 2.74 (s, 6H, ortho CH_3), 2.34 (s, 6H, ortho CH_3), 2.23 (s, 3H, para CH_3), 1.91 (s, 3H, para CH_3). $^{13}\text{C}\{^1\text{H}\}$ NMR (C_6D_6): δ 305.34 (m, Ru=*CHPh*), 219.57 (d, Ru- $\text{C}(\text{N})_2$, $J_{\text{CP}} = 92$ Hz), 151.69 (d, $J_{\text{CP}} = 4$ Hz), 139.68, 138.35, 138.10, 138.97, 137.78, 135.89, 135.21, 135.13, 131.96, 131.65, 131.36, 130.47, 129.83, 129.59 (d, $J_{\text{CP}} = 2$ Hz), 129.15, 128.92, 128.68, 128.00, 52.11 (d, $J_{\text{CP}} = 4$ Hz), 51.44 (d, $J_{\text{CP}} = 2$ Hz), 21.67, 21.35, 21.04, 19.21. Anal. Calcd for $\text{C}_{46}\text{H}_{47}\text{N}_2\text{Cl}_2\text{PRu}$: C, 66.50; H, 5.70; N, 3.37. Found: C, 66.82; H, 5.76; N, 3.29.

(IMesH₂)(O^tBu)₂Ru=CHPh (11). Complex **3** (7.5 mg, 0.010 mmol) and KO^tBu (3 mg, 0.027 mmol) were combined in C_6D_6 (0.6 mL) in an NMR tube under nitrogen. The reaction mixture was allowed to stand for 15–20 min, during which time a color change from green to dark red was observed, and NMR spectra were recorded after 30 min. ^1H NMR (C_6D_6): δ 16.56 (s, 1H, Ru=*CHPh*), 7.63 (d, 2H, ortho *CH*, $J_{\text{HH}} = 7$ Hz), 7.2–7.1 (multiple peaks, 3H, meta *CH* and ortho *CH*), 6.97 (s, 4H, Mes *CH*), 3.43 (s, 4H CH_2CH_2), 2.59 (s, 12H, ortho CH_3), 2.29 (s, 6H, para CH_3), 1.18 (s, 18H, ^tBu).

Tp(IMesH₂)(Cl)Ru=CHPh (12). KTp (87 mg, 0.34 mmol) and complex **3** (125 mg, 0.17 mmol) were combined in CH_2Cl_2 (10 mL) and stirred for 1 h. Pentane (20 mL) was added to precipitate the salts, and the reaction was stirred for an additional 30 min and then cannula filtered. The resulting bright green solution was concentrated, and the solid residue was washed with pentane (2 × 10 mL) and methanol (2 × 10 mL) and dried under vacuum to afford **12** (84 mg, 66% yield) as an analytically pure green powder. ^1H NMR (CD_2Cl_2): δ 18.73 (s, 1H, Ru=*CHPh*), 7.87 (d, 1H, Tp, $J_{\text{HH}} = 2.4$ Hz), 7.41 (d, 1H, Tp, $J_{\text{HH}} = 2.1$ Hz), 7.35–7.30 (multiple peaks, 3H, Tp and para *CH*), 7.08 (d, 1H, Tp, $J_{\text{HH}} = 1.5$ Hz), 6.82 (br. s, 5H, Mes *CH*, ortho *CH* and meta *CH*), 6.24 (br. s, 3H, Mes *CH*), 6.16 (t, 1H, Tp, $J_{\text{HH}} = 1.8$ Hz), 5.95 (d, 1H, Tp, $J_{\text{HH}} = 1.5$ Hz),

5.69 (t, 1H, Tp, $J_{\text{HH}} = 2.4$ Hz), 5.50 (t, 1H, Tp, $J_{\text{HH}} = 1.8$ Hz), 3.77 (br. d, 4H, CH_2CH_2), 2.91–0.893 (br. multiple peaks, 18H, ortho CH_3 , para CH_3). $^{13}\text{C}\{^1\text{H}\}$ (CD_2Cl_2): δ 324.29 (m, Ru=*CHPh*), 220.57 (s, Ru- $\text{C}(\text{N})_2$), 151.50, 146.08, 145.39, 142.07, 137.94, 136.57, 134.41, 133.18, 130.60 (br), 129.55, 127.98, 106.41, 105.19, 104.51, 53.77 (br), 21.26, 20.32 (br). Anal. Calcd for $\text{C}_{37}\text{H}_{42}\text{N}_3\text{ClBRu}$: C, 59.56; H, 5.67; N, 15.02. Found: C, 59.20; H, 5.67; N, 14.72.

Kinetics of the Reaction of 2 with C₃D₅N. In a cuvette fitted with a rubber septum, a solution of **2** (0.88 mM) in toluene (1.6 mL) was prepared. This solution was allowed to thermally equilibrate in the UV-vis spectrometer at 20 °C. Neat pyridine-*d*₅ (25–100 μL) was added via microsyringe, and the reaction kinetics was followed by monitoring the disappearance of starting material (502 nm). For each run, the data were collected over five half-lives and were fitted to a first-order exponential. Typical R^2 values for the exponential curve fits were greater than 0.999.

X-ray Crystal Structure of 3. Crystal, intensity collection, and refinement details²⁹ are summarized in Table 1. The selected crystal was mounted on a glass fiber with Paratone-N oil and transferred to a Bruker SMART 1000 CCD area detector equipped with a Crystal Logic CL24 low-temperature device. Data were collected with ω -scans at seven φ values and subsequently processed with SAINT.³⁰ No absorption or decay corrections were applied. SHELXTL³⁰ was used to solve (by direct methods and subsequent difference Fourier maps) and to refine (full-matrix least-squares on F^2) the structure. There are two molecules in the asymmetric unit. All non-hydrogen atoms were refined anisotropically; the hydrogen atoms were placed at calculated positions with U_{iso} values based on the U_{eq} of the attached atom. Pertinent bond lengths and angles for one molecule are presented in Table 2.

Acknowledgment. Lawrence Henling and Michael Day are acknowledged for the X-ray crystallographic study described herein. The authors would like to thank the NSF for generous funding of this research. J.A.L. thanks the NIH for a postdoctoral fellowship.

Supporting Information Available: Experimental data for the synthesis of all new complexes and crystallographic data (labeled drawings, table of atomic coordinates, complete bond distances and angles, and anisotropic displacement parameters) for complex **3**. This material is available free of charge via the Internet at <http://pubs.acs.org>.

OM010599R

(29) The Crystallographic Information File (CIF) for **3** has been deposited with the Cambridge Crystallographic Data Centre as supplementary publication no. CCDC 143577. Copies of the data can be obtained, free of charge, on application to CCDC, 12 Union Road, Cambridge CB2 1EZ, UK, (fax: +44 1223 336033 or e-mail: deposit@ccdc.cam.ac.uk). Structure factors are available from the authors via e-mail: xray@caltech.edu.

(30) Bruker 1999 SMART, SAINT, and SHELXTL; Bruker AXS Inc.: Madison, WI.